

Aggregation - Disaggregation Cycles in ERA 5 Reanalysis

VIJIT MAITHEL^{a,b}, LARISSA BACK^b

^a Cooperative Institute for Research in Environmental Sciences, University of Colorado Boulder, Boulder, CO

^b University of Wisconsin-Madison

ABSTRACT: Understanding convective aggregation is very important for understanding tropical climate and climate sensitivity. However, we still lack a full understanding of how aggregation evolves in the real world or what real world phenomena can be the counter parts to the phenomena of self-aggregation observed in idealized models. In this study, we apply the moist static energy (MSE) variance budget framework to ERA 5 reanalysis data to study the evolution of large-scale aggregation in the real world. Our novel phase space diagnostics highlight the cyclic nature of real world aggregation, compared to the quasi-stationary features of the idealized aggregated state. Therefore, we visualize real world aggregation to evolve in the form of anomalies evolving about a mean state forming aggregation - disaggregation cycles. We find horizontal advection to play the primary role in determining when the domain aggregates or disaggregates in the real world. In contrast, all advective, radiative and surface flux feedbacks are found important for determining the magnitude of the aggregation anomalies. Surface fluxes and horizontal advection tend to dampen aggregation anomalies, while radiative fluxes and vertical advection tend to amplify aggregation anomalies. Looking deeper into the advection terms, we find that changes in vertical advection are dominated by an enhanced low level subsidence over the dry columns during the more aggregated states which creates an anomalous drying tendency for the dry columns. In contrast, horizontal advection changes are found to be dominated by increased moisture advection out of the moist columns with stronger aggregation.

SIGNIFICANCE STATEMENT: The purpose of this study is to characterize and understand the evolution of large-scale convective aggregation in the real world through reanalysis data. While most previous observational studies have focused on evolution of clouds and cloud populations with aggregation, we focus on the energetics and the impact of aggregation on redistributing moisture throughout the domain. Our framework highlights that aggregation can be visualized as a continuously occurring cyclic feature at large-scales in the tropics. Further, our work provides a deeper insight into the changes in large-scale circulation that accompany aggregation, and characterizes the similarities and differences between the different regions in the tropics.

1. Introduction

Convective aggregation is generally used to refer to clustering of clouds (and hence convection) in a non random manner in a domain. Broadly, it can be a result of non-uniform boundary conditions acting on the domain (external factors), or because of feedbacks between convection, moisture, and radiation (internal factors). Idealized numerical models with uniform boundary conditions have been extensively used to study the characteristics of convective aggregation driven solely by these internal feedbacks, also referred to as convective self-aggregation (Bretherton et al. 2005; Held et al. 1993). In contrast, convection in the real world can additionally also aggregate because of the presence and evolution of non-uniform boundary conditions,

termed as convective aggregation. It is not completely clear what role or relevance the mechanisms behind self aggregation play when it comes to aggregation in the real world (review by Holloway et al. 2017). However, there are some key characteristics that have been identified in how both self aggregation and aggregation can impact the spatial domain. Studies have showed that the domain consistently becomes drier, outgoing long wave radiation (OLR) increases, and spatial gradients of column water vapor in the domain increase as it gets more aggregated, both in idealized models (Bretherton et al. 2005; Wing and Emanuel 2014; Wing and Cronin 2016; Holloway and Woolnough 2016, etc.), and observations (Tobin et al. 2012; Tsai and Mapes 2022; Stein et al. 2017; Bony et al. 2020, etc.). This robust impact of aggregation on the large scale environment, combined with the dependence of aggregation on sea surface temperatures (SST) (Cronin and Wing 2017; Coppin and Bony 2015) make understanding convective aggregation extremely important to understanding climate sensitivity (review by Wing 2019).

To understand links between aggregation and self aggregation, we first need to understand the nature of convective aggregation in the real world, and how it differs from the model world. Convection in idealized models starts off from a completely disaggregated state with randomly distributed convection. Then with time, the domain slowly transitions to a new equilibrium state with aggregated convection which stays aggregated for the remainder of the simulation. In contrast, in real world, convection will already be in a somewhat aggregated state due to the presence of external boundary conditions and feedbacks from previ-

Corresponding author: Vijit Maithel, vijit.maithel@noaa.gov

ous convective events. However, the extent of aggregation can change with time, and convection also disaggregates. This will result in cycles of aggregation and disaggregation. Such cycles of changing extent of aggregation can also be observed in some idealized simulations once the aggregated state has been reached. However, these have not been studied systematically in terms of what leads to such variability, and more focus has been put on understanding what initiates and maintains the overall aggregated state.

To measure the extent of aggregation in observations, previous studies have used a variety of cloud clustering based metrics. Each of these metrics, in some way or the other, combines different cloud properties from satellite observations to quantify cloud clusters so as to act as an aggregation metric. Some prominent metrics in use are the Simple Convective Aggregation Index (SCAI, Tobin et al. 2012), organization index I_{org} (Tompkins and Semie 2017), the Morphological Index of Convective Aggregation (MICA, Kadoya and Masunaga 2018) etc. However, there can be some concerns about how well these metrics correlate with larger scale convective organization in the real world. For example, Sakaeda and Torri (2022) show that self aggregation based cloud metrics do not necessarily correlate well with the Madden Julian Oscillation (MJO) phase index. They show that many metrics are unable to show an increase in aggregation during the active MJO phase and some even show that convection becomes less aggregated during the MJO active phase. They highlight that these discrepancies primarily arise because of how these metrics can be biased towards particular cloud properties by construction (like cloud clusters becoming larger or clusters becoming fewer) and individually may not fully capture all characteristics of cloud evolution in real world.

Such factors make it difficult to compare self aggregation in idealized models with aggregation in the real world directly. However, since both models and observations have showed consistent and strong impacts on the large scale environment (Wing 2019), there is potential to define aggregation based on the state of the large scale environment itself. A particularly strong, robust and easy to track metric for doing so is the spatial variability of column water vapor. Motivation for using this metric is twofold. One, the column water vapor distribution has been shown to vary with aggregation significantly in both observations (Lebsock et al. 2017; Tsai and Mapes 2022) and models (Bretherton et al. 2005; Wing and Emanuel 2014). Two, empirical evidence shows a strong dependence of precipitation on a critical moisture threshold (Bretherton et al. 2004) and the existence of sharp water vapor margins for the Inter-Tropical Convergence Zones (ITCZ) (Mapes et al. 2018). This suggests that convection, aggregation, and the distribution of column moisture in the tropics are strongly interconnected with each other. Aggregation can impact the distribution of water vapor in the tropics and vice-versa.

This also provides strong support to the idea that self aggregation mechanisms can be relevant for understanding convective variability that is driven by changes in moisture in the real world (Adames-Corraliza and Mayta 2023; Tsai and Mapes 2022). Other recent studies have highlighted such moisture driven modes of convective variability being observed ubiquitously throughout the tropics (Inoue and Back 2017), and the mechanisms behind them to be very inherent to how convection interacts with the large scale environment (Inoue et al. 2021; Maithel and Back 2022). Lebsock et al. (2017) have used and verified that the spatial variance of column water vapor can be used as a metric for aggregation using satellite data.

All together, this suggests that studying the evolution of moisture can be an indirect way of tracking aggregation. Owing to the weak temperature gradient approximation (WTG) (Sobel et al. 2001), the evolution of moisture can be studied using moist static energy (MSE) budgets. While the MSE budget (Eq. 1) has been extensively used to study moisture driven convective variability, the MSE variance budget (Eq. 2) (Wing and Emanuel 2014) has been extensively used to study self aggregation and for tropical cyclone diagnostics (Wing and Emanuel 2014; Coppin and Bony 2015; Holloway and Woolnough 2016; Wing et al. 2019; Dirkes et al. 2023, etc.).

$$\frac{\partial \langle h \rangle}{\partial t} = \text{VADV} + \text{HADV} + \langle Q_R \rangle + SF + \text{Res} \quad (1)$$

$$\begin{aligned} \frac{1}{2} \frac{\partial \langle h \rangle'^2}{\partial t} = & \langle h \rangle' \text{VADV}' + \langle h \rangle' \text{HADV}' \\ & + \langle h \rangle' \langle Q_R \rangle' + \langle h \rangle' SF' + \langle h \rangle' \text{Res}' \end{aligned} \quad (2)$$

$$\text{VADV} = - \langle \omega \partial h / \partial p \rangle$$

$$\text{HADV} = - \langle \mathbf{v} \cdot \nabla h \rangle$$

In Eq. 1 and 2, $\langle \dots \rangle$ represents mass weighted vertical column integral from the surface to 100hPa, $'$ represents anomaly compared to the domain mean, h represents MSE, ω represents vertical velocity in pressure coordinates, \mathbf{v} is the horizontal wind vector, VADV and HADV stand for vertical and horizontal advection respectively, $\langle Q_R \rangle$ are the column radiative fluxes, SF are the surface sensible and latent heat fluxes, and Res stands for the residual term.

The MSE variance budget framework (Wing and Emanuel 2014) makes use of the observation that self aggregation results in redistribution of moisture and MSE within the domain to resemble a bimodal distribution with anomalously moist and dry columns instead of being more uniformly distributed (Bretherton et al. 2005). This implies an increase in the value of the spatial variance of MSE with aggregation. Furthermore, the MSE variance budget (Eq. 2) can be used to measure how different processes contribute to the increase or decrease of MSE variance. It

is derived by multiplying the the spatial anomalies of the terms in Eq. 1 with anomalous column MSE at each time instant. A positive variance budget term represents that the anomalously moist columns in the domain tend to further moisten as a result of that process or anomalously dry columns will tend to further dry up. This implies that the term tends to act as a positive feedback on column MSE anomalies. Since amplifying or sustaining existing MSE anomalies help aggregation, positive feedbacks on MSE anomalies support aggregation. Consequently, a negative variance budget term signifies that the term acts as a negative feedback on column MSE anomalies, and does not support aggregation.

Using the MSE variance budget, idealized modeling studies found the positive feedback of radiative fluxes on column MSE anomalies to be the dominant mechanism responsible for initiation as well as maintenance of self aggregation (Wing et al. 2017; Pope et al. 2021, 2023). Their role in helping maintain the self aggregated state once it has already aggregated can be particularly relevant for the real world. This is supported in observations which showed that at large scales, anomalous column radiative fluxes vary linearly with anomalous column moisture with a positive slope (Su and Neelin 2002; Inoue and Back 2017). This implies that positive moisture anomalies are linked with anomalous moistening tendency or negative moisture anomalies are linked with anomalous drying tendency, that is, radiative fluxes act as a positive feedback on MSE anomalies. Moreover, the positive slope also implies that the feedback is expected to get stronger with larger anomalies. However, this only shows that radiative anomalies strongly covary with MSE or moisture anomalies. This does not tell us about the causality, whether the larger anomalies occur when the positive feedback from radiative fluxes becomes stronger or vice versa. In other words, are changes in MSE anomalies or changes in aggregation driven by changes in radiative feedbacks? That will be shown if the contribution from the radiative term also covaries positively with MSE tendency or MSE variance tendency. Many recent studies looking at evolution of the aforementioned moisture driven convective variability modes in observations have found the tendencies in column MSE to be driven strongly by advection instead of radiation, with radiation being important for maintenance (Inoue et al. 2021; Maithel and Back 2022; Mayta and Adames-Corraliza 2023).

This brings us to the main question being addressed in this study. Does convection in the real world aggregate/disaggregate whenever the positive feedback from radiative fluxes strengthens/ weakens respectively? Or do radiative feedbacks only contribute to determining the extent of aggregation whereas advective processes determine when things aggregate and disaggregate? We hypothesize that advection of MSE plays a large role in driving aggregation disaggregation cycles in observations and our hypothesis is

supported by the analysis in this paper. We use the spatial variance of MSE as our metric of aggregation.

The rest of this paper is structured as follows. Section 2 describes the data set being used and how the variance budget calculation is set up. It also introduces the novel variance phase space that we will use as our diagnostic framework. Section 3 presents the main results from the study, while section 4 presents the summary and discussion.

2. Data and Methods

We use ERA 5 data (Hersbach et al. 2020) as our best guess for what is happening in the real world for this study. Temperature, humidity, winds, radiation, sensible and latent heat surface fluxes are used from ERA 5 to compute the column integrated MSE and column integrated MSE budget time series at each grid point. Column integrated quantities are computed by taking the vertical integral across 27 vertical levels between 1000hPa and 100hPa. Further, the MSE variance budget terms are computed over four large domain boxes, each corresponding to the four main tropical ocean basins: an Indian Ocean (IO) box spanning between 10° S - 5° N and 55° - 95° E, a Western Pacific (WP) box spanning 5° S - 10° N and 150° - 180° E, an Eastern Pacific (EP) box spanning 0° - 15° N and 195° - 265° E, and an Atlantic Ocean (AO) box spanning 0° - 15° N and 315° - 340° E. We use data at horizontal resolution of $0.5^{\circ} \times 0.5^{\circ}$ and a time resolution of 6 hr from 1980-2019 within each box. The MSE budget time series at each grid point is further passed through a 24 hr running mean filter to remove diurnal variability from the data.

The domains we use are much larger than the $10^{\circ} \times 10^{\circ}$ or $5^{\circ} \times 5^{\circ}$ boxes used to evaluate the cloud based aggregation metrics in previous studies. In this study, we are focusing on defining aggregation through its impact on the large scale distribution of MSE. Hence the need for larger domain size. Because of the larger domain size, the domains can be expected to be closer to radiative convective equilibrium (RCE) more frequently (Jakob et al. 2019). Also this shifts the focus to being on convective features and aggregation at larger scales (like the ITCZ) which evolves more slowly at sub-seasonal timescales making it more comparable to self aggregation in idealized models. It should be noted that the majority of the existing literature on convective aggregation in the real world is instead focused more at cloud organization at meso-scales.

The MSE variance budget terms are calculated as follows from the MSE budget time series data. First, for each grid point, the spatial anomaly of column MSE and each of the budget terms is computed by subtracting the respective domain mean at each time step. Then the MSE budget term anomaly is projected onto the column MSE anomaly for every point. Finally, a domain mean of the projected term is calculated, creating a one dimensional

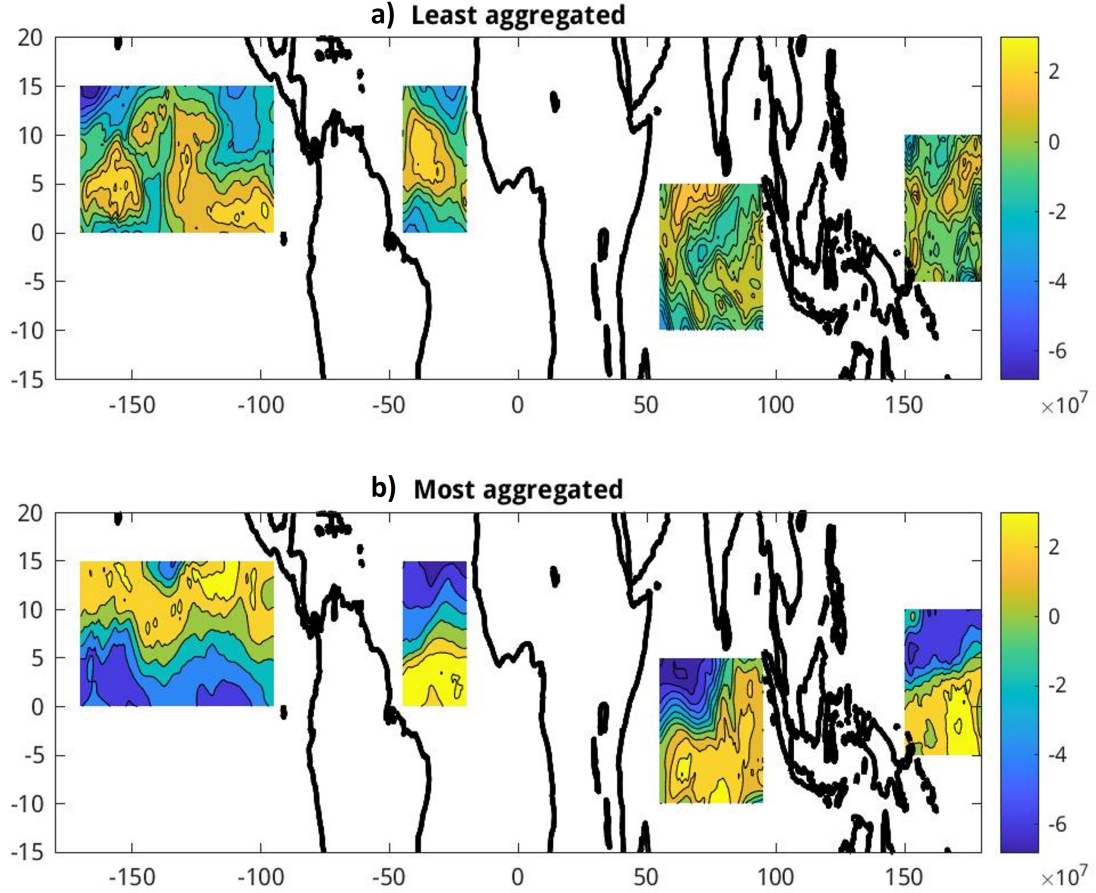


FIG. 1. Spatial structure of the column MSE anomalies (J/m^2) in the four ocean basin domain being studied when a) each domain is least aggregated, and b) domain is most aggregated. Both a) and b) follow the same colorbar.

time series to represent each term in equation 1 in each of the four ocean boxes. Figure 1 shows the spatial distribution of column MSE anomalies when the domain mean MSE variance is low (top), and when the domain mean MSE variance is high (bottom) for each of the four boxes. A strongly aggregated domain in this framework looks like a strong latitudinal ITCZ band with sharp margins.

We propose to use a novel MSE variance based phase space to visualize and track the evolution of domain mean MSE variance. The phase space is formed by taking domain mean MSE variance on the x-axis and the tendency of the domain mean MSE variance on the y-axis. While the x-axis physically corresponds to the extent or degree of aggregation in the domain, the y-axis represents the process: whether it is undergoing aggregation or disaggregation. A schematic of an idealized aggregation-disaggregation cycle is shown in fig. 2a. The arrows depict the expected trajectory on the phase space as the domain aggregates (left to right) and disaggregates (right to left), together forming the cycle.

The main idea is that the phase space allows us to visualize the different phases of this cycle and look at how the contributions from the various terms in Eq. 2 changes across the different phases. More and less aggregated phases are the right and left halves respectively, and aggregating and disaggregating phases are the top and bottom halves respectively. This picture encourages one to think of large-scale aggregation in the real world as a transient cyclic process and not as a change in the mean state.

We also choose to normalize the MSE variance and MSE variance budget terms so that the two phase plane axes have similar magnitudes. We do so by dividing the domain mean MSE variance time series for each domain by the maximum mean MSE variance observed in that domain, and the domain mean MSE variance tendency by the maximum absolute value of the domain mean MSE variance tendency in the domain. As a result, the x-axis on the phase plane has a range between 0 and 1, and y-axis ranged between -1 to 1. Other MSE variance budget terms

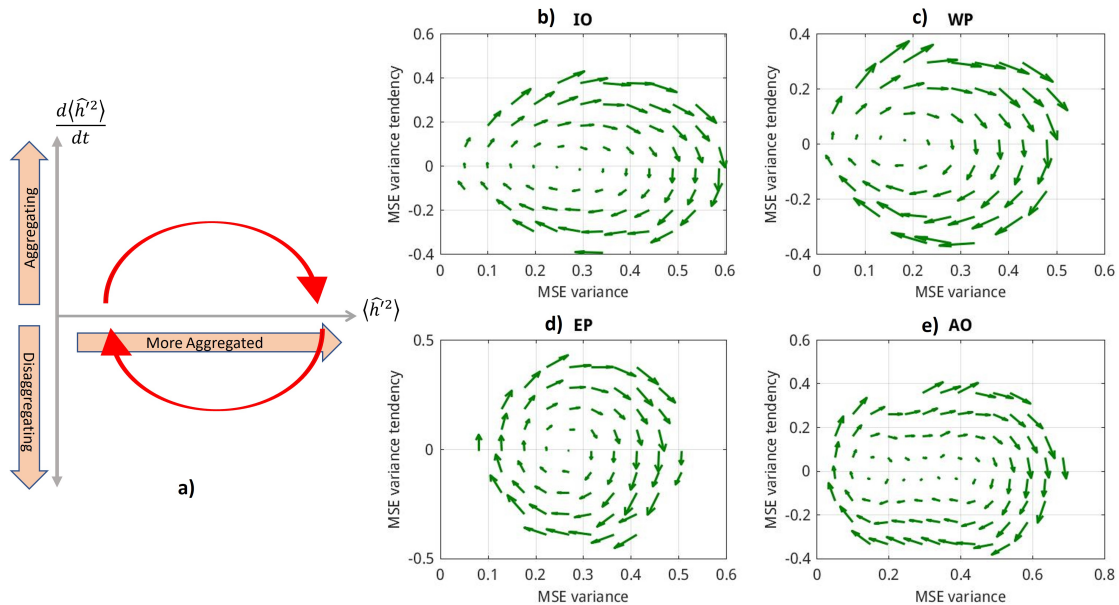


Fig. 2. a) A simple schematic of the MSE variance phase space and the idealized aggregation - disaggregation cycle. The X-axis is the domain mean MSE variance, and y-axis is the tendency of domain mean MSE variance. Red arrows represent what a typical aggregation - disaggregation cycle would look like. b)-e) vector plot showing the actual evolution on the MSE variance phase plane in reanalysis data for the four ocean basins - IO, WP, EP, AO respectively. For easier visualization, the phase plane has been divided into 400 equally spaced bins (20 along each axis) and bin mean values have been plotted. Only bins with more than 100 samples are shown.

from Eq. 2 are normalized by the same maximum MSE variance tendency value.

3. Results

First we verify that the cyclic variability on the phase space, expected in figure 2a is also observed in the reanalysis data. To do so, we plot a phase portrait for our two dimensional phase space showing vectors corresponding to the direction of evolution on the phase plane. The vectors are computed by first computing the time derivatives of the domain mean MSE variance and domain mean MSE variance tendency at each time step. Then, the phase plane is divided into 400 small rectangular bins (20 equally spaced bins along each axis). Then we compute the bin mean time derivative of the MSE variance (vector magnitude along x-axis) and the bin mean time derivative of the MSE variance tendency (vector magnitude along y-axis) for each bin. The resulting bin mean vectors for each ocean basin are plotted in fig. 2 b-e. Only bins with more than 100 samples are plotted. We observe that the cyclic signal as visualized in the simple schematic in fig. 2a is reproduced very clearly in all ocean basins. This signifies that extent of large scale aggregation indeed varies cyclically everywhere throughout the tropics in the form of these aggregation - disaggregation cycles.

Before we delve deeper into looking at this cyclic behavior, we characterize the mean state of aggregation in

reanalysis by plotting the mean value of the MSE variance budget terms averaged over the full time series. Figure 3 shows the mean MSE variance budget terms for each ocean basin. Since the mean MSE variance tendency is zero in this figure, these values can be compared qualitatively with those during the equilibrium part of the idealized model simulations when the domain has already reached an aggregated and quasi-stationary equilibrium state.

From figure 3, we observe that the column radiative and surface fluxes act as mean positive and negative feedbacks on column MSE anomalies respectively in all ocean basins. Hence, mean radiative fluxes support aggregation and mean surface fluxes resist aggregation. This is broadly consistent with results in Pope et al. (2023) who thoroughly analyzed the diabatic flux feedbacks in the different model runs part of the Radiative-Convective Equilibrium Model Intercomparison Project (RCEMIP; Wing et al. 2018, 2020). Radiative fluxes act as a positive feedback due to longwave interactions with high clouds, and shortwave absorption by water vapor in moist regions dominating the variance from radiative fluxes as per these idealized modeling studies (Pope et al. 2023). Regarding surface flux feedbacks, we observe that in ERA 5 they tend to resist aggregation during all phases of the cycle in all ocean basins. A possible hypothesis for this could be that surface fluxes are dominated by negative feedback processes which tend to moisten dry regions compared to positive feedback processes like the wind driven sur-

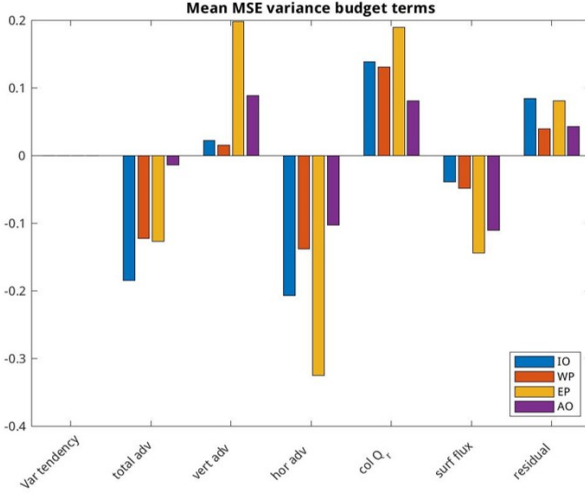


FIG. 3. Bar plot showing the mean MSE variance budget terms from Eq. 2 for the full time series. A residual term is also computed to accommodate the fact that MSE budget is not exactly closed in ERA5 data. Different colors correspond to different ocean basins with IO in blue, WP in orange, EP in yellow, and AO in purple

face heat exchange feedback (WISHE) which will tend to moisten the moist regions. Such negative feedback processes in dry regions could be related to increased air-sea enthalpy disequilibrium (Wing and Emanuel 2014) and is consistent with Bretherton and Khairoutdinov (2015) that found anomalous surface fluxes dominated by increases in dry intrusions.

Vertical advection displays large qualitative differences between the different basins. While over Eastern Pacific and Atlantic Ocean basins, vertical advection has a strong mean positive feedback on MSE anomalies, over Indian Ocean and Western Pacific the mean feedback is closer to zero and smaller than the residual. This suggests that the mean overturning circulation does not transfer MSE effectively from moist to dry regions by itself when contribution from horizontal advection of MSE is not being included. This is interesting because this is the opposite of what will be expected from a traditional Hadley cell picture for the mean tropical circulation which helps transport excess energy from tropics towards subtropics due to upper level divergence in the ascending branch of the Hadley cell. A possible explanation for such inter basin differences could be related to differences in vertical motion profile shape. Back and Bretherton (2006); Back et al. (2017) showed that climatological vertical motion profile shapes being more bottom heavy in Eastern pacific and Atlantic Ocean can lead to negative gross moist stability values in the region. Further we observe that horizontal advection acts a mean negative feedback on MSE anomalies in all ocean basins. This motivates thinking of horizontal advection as a mixing term which physically tends to reduce MSE gradients in the domain. It is interesting to note that total advection acts

as a overall negative feedback on MSE anomalies (with the exception of Atlantic basin) suggesting that horizontal advection feedbacks dominate vertical advection feedbacks. While most models do not compute the vertical and horizontal advection variance terms explicitly to compare with reanalysis here, Pope et al. (2023) do find total advection to act as a net negative feedback in RCEMIP model runs once the models have reached an aggregated state.

a. Contribution to maintenance and propagation of MSE variance anomalies averaged over the complete cycle

As mentioned previously, we are interested in understanding what drives cyclic behavior in aggregation. We are particularly focused on how the MSE variance budget terms vary during different phases of the cycle. One way to do so is to understand how each of the budget terms in Eq. 2 co-vary with MSE variance (in the x-direction) and with MSE variance tendency (in the y-direction). This is same as asking how each term contributes to maintenance and propagation of these cycles respectively. This can be evaluated by projecting the MSE variance budget (Eq. 2) onto the appropriate terms and computing the total projection for the full time series as given by the equations below.

$$M_x = \frac{\left\{ \left| \hat{X} \cdot \overline{\langle h \rangle'}^2 \right| \right\}}{\left\{ \left| \overline{\langle h \rangle'}^2 \right| \right\}} \quad (3)$$

$$P_x = \frac{\left\{ \left| \hat{X} \cdot \overline{\left| \frac{\partial \langle h \rangle'}{\partial t} \right|^2} \right| \right\}}{\left\{ \left| \overline{\left| \frac{\partial \langle h \rangle'}{\partial t} \right|^2} \right| \right\}} \quad (4)$$

In equations 3 and 4, X represents a term from the MSE variance budget in Eq. 2, $\overline{\dots}$ represents the domain mean, $|\dots|$ represents the time anomaly, and $\{\dots\}$ represents the mean of the underlying term across the full time series. This is analogous to the maintenance and propagation terms calculated in Andersen and Kuang (2012) for the MSE budget. The propagation term (Eq. 4) represents whether the budget term anomalies are the same sign as the MSE variance tendency anomalies or the MSE variance tendency (since mean tendency is zero from fig. 3). The maintenance term (Eq. 3) represents how the budget terms vary with the domain being anomalously more or less aggregated. Therefore, while the value of the MSE variance budget term itself represents whether the particular process acts as a positive or negative feedback on column MSE anomalies, the maintenance and propagation projections represent how the strength of that feedback changes when the domain is anomalously more/ less aggregated, and while it is in the process of aggregating/ disaggregating respectively.

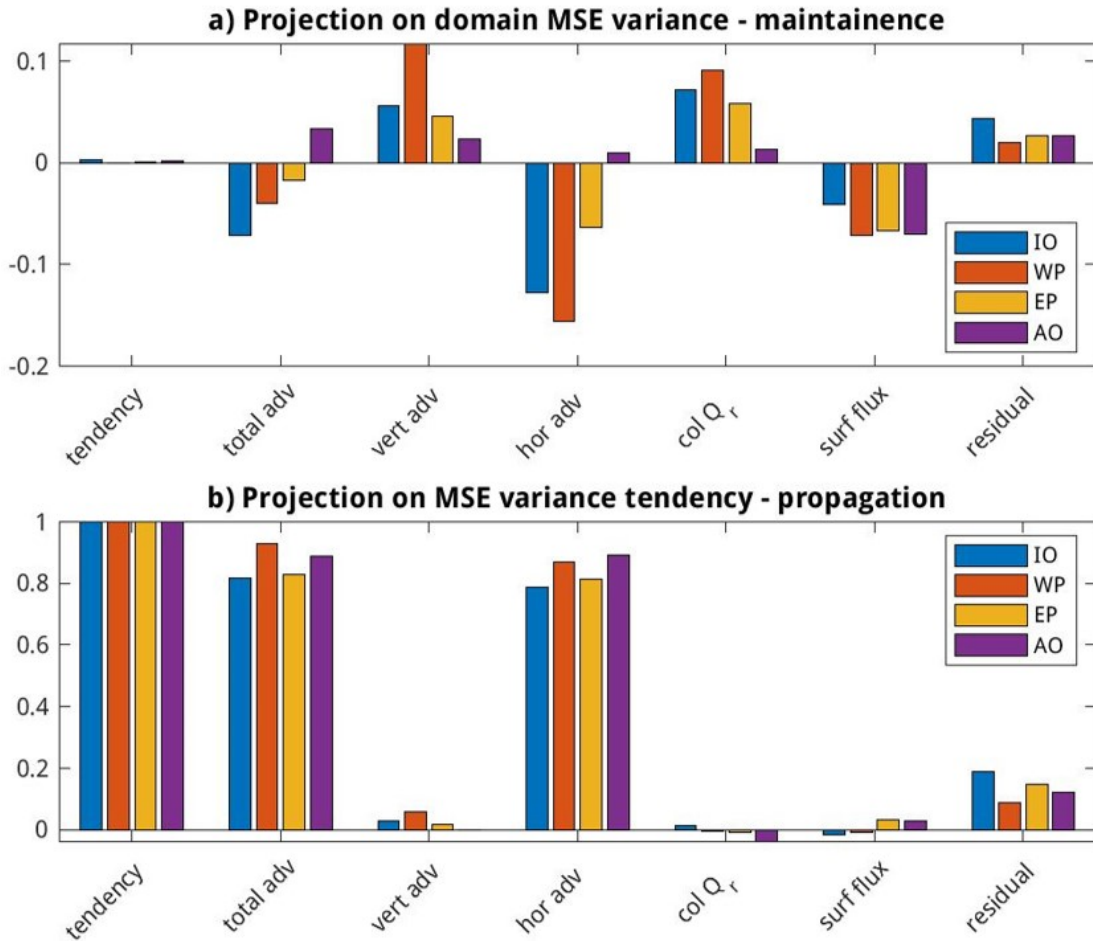


FIG. 4. Bar plot showing the contribution of each MSE variance budget term from Eq. 2 (including residual) to a) Maintenance of MSE variance - computed as per Eq. 3, and b) propagation of MSE variance - computed as in Eq. 4. Different colors correspond to different ocean basins with IO in blue, WP in orange, EP in yellow, and AO in purple

It should be noted that this notion of the maintenance term primarily refers to maintenance of aggregation anomalies during the aggregation-disaggregation cycle. This is different from when previous studies have used the term maintenance which deals more with whether a process helps maintain a mean aggregated state compared to a completely disaggregated state. In other words, maintenance in previous studies is related to the mean value of the MSE variance budget term (fig. 3), while here maintenance corresponds to how anomalies of the variance budget term correlates with anomalous domain MSE variance. In the rest of this paper, by maintenance of aggregation, we will refer to maintenance in the context of aggregation-disaggregation cycles and whether a process is maintaining an aggregation anomaly in the reanalysis. Since this metric measures how things are changing with aggregation anomalies, it is also a quantification of the feedback on aggregation. However to avoid any confu-

sion about the context in which the term feedback is being used, we'll use the term feedback only in context of MSE anomalies. Feedback on aggregation will be referred to as positive or negative contribution to maintenance of aggregation anomalies.

Figure 4 shows the projections of each term contributing to the maintenance and propagation of the cycles. Figure 4a shows that vertical advection and column radiation fluxes have a positive contribution to maintenance while horizontal advection and surface fluxes have a negative contribution to maintenance of aggregation anomalies. A positive contribution to maintenance implies that the variance budget term varies such that it anomalously favors further aggregation when the domain is more aggregated, or it anomalously supports disaggregation when the state is already less aggregated. This can happen due to multiple reasons depending on whether the particular variance budget term has a positive or negative feedback, that is,

whether it supports or resists aggregation respectively. For example, consider a positive feedback on MSE anomalies. A positive maintenance contribution means a stronger support to aggregation as the domain becomes more aggregated. This could be because of its tendency to moisten the moist columns more strongly, or dry the dry columns more strongly as the domain becomes more aggregated. In the opposite manner, for a negative feedback on MSE anomalies, a positive maintenance contribution means a weaker resistance to aggregation as the domain becomes more aggregated. This could be because of its tendency to dry the moist columns less strongly, or moisten the dry columns less strongly as the domain gets more aggregated. In contrast, a negative contribution to maintenance represents that the MSE variance budget term varies such that it favors anomalous disaggregation when the domain is more aggregated or it supports anomalous aggregation in the domain when it is less aggregated. Similar to the case for positive maintenance terms, a negative maintenance contribution can also be a result of different pathways depending on whether the term is behaving like a positive or negative feedback. Which pathway is in action for which term is discussed more in subsequent sections.

Overall, we see some amount of qualitative agreement between the different ocean basins even though there are also some stark quantitative differences. For example, surface fluxes have a strong negative contribution to maintenance consistently throughout the tropics. Vertical advection and column radiation have the same sign of impact on maintenance in all ocean basins - a positive contribution - but these terms show larger basin-to-basin variations in magnitude. Horizontal advection here seems to be an outlier in the sense that the sign of the term also seems to change between the ocean basins in addition to its magnitude. This is discussed further in the next subsection.

The propagation term shown in fig. 4b shows that almost all of the contribution to propagation of aggregation cycles comes from horizontal advection in all ocean basins. A positive contribution to propagation means that the MSE variance budget term positively covaries with tendency. This will happen if the domain mean MSE variance tendency has the same sign as the contribution to the tendency from the anomalies in the budget term. That is, the overall domain tends to aggregate or disaggregate when the specific contribution from the particular term also tends to anomalously support aggregation or disaggregation respectively. In contrast, a negative contribution to propagation denotes that the anomalous variance budget term is of the opposite sign to the total MSE variance tendency and the particular budget term tends to be disaggregating the system when overall it is aggregating or vice versa. A zero value denotes that there is no specific pattern between how the two co vary. It is observed that the propagation of the aggregation-disaggregation cycles is almost exclu-

sively because of horizontal advection in all ocean basins with other terms being close to zero.

This horizontal advection contribution to propagation is significant because it implies that statistically the diabatic terms do not play a major role in determining when the domain aggregates or disaggregates. We expect that while the contribution from diabatic terms may be non zero for individual cycles, when averaging over multiple cycles, we observe that they do not have a specific influence on how the existing state of aggregation will change. This is potentially important for understanding how the frequency of aggregation-disaggregation cycles might change in the real world with climate change, and suggests that understanding the change in advective feedbacks will be more important to understand this aspect of aggregation.

b. Contribution to maintenance and propagation of MSE variance anomalies during different phases of the cycle

Because the values calculated as per Eq. 3 and 4 include taking a mean over the full time series, it represents the contribution of each term averaged over all the different phases of the cycle. However we can understand the contribution of each term during the different phases by using the MSE variance phase plane (figure 2a) to only average over the same phase bins across different cycles.

Figure 5 shows contours of the bin mean values for each of the MSE variance budget terms in Eq. 2 for the Indian Ocean basin on the phase plane. The contours represent how each term in the variance budget varies across the different phases of the aggregation-disaggregation cycles. The contours show the full variability in strength of the feedback that goes into computing the maintenance and propagation metric in the previous subsection.

We can interpret the maintenance and propagation terms from the previous subsection as how the budget term vary along the x and y axes respectively. Since variance from horizontal advection is the only term which varies in magnitude along the y-direction (fig. 5b), it is the only contributor to propagation in fig. 4b. The three remaining terms vary primarily along the x-direction, making their contribution to propagation close to zero. Variance from vertical advection, column radiation, and surface fluxes do not vary much between the aggregating and disaggregating phase for a given amount of aggregation. This ties back in with our initial hypothesis that diabatic terms can not sufficiently be the driving force behind the observed aggregation disaggregation cycles. Instead we observe that advection terms vary with the y-axis on the phase plane indicating that advection, particularly horizontal advection is important for driving these aggregation-disaggregation cycles.

We can further observe that vertical advection (fig. 5a) and column radiation fluxes (fig. 5d) become stronger positive feedbacks when the domain is more aggregated, and

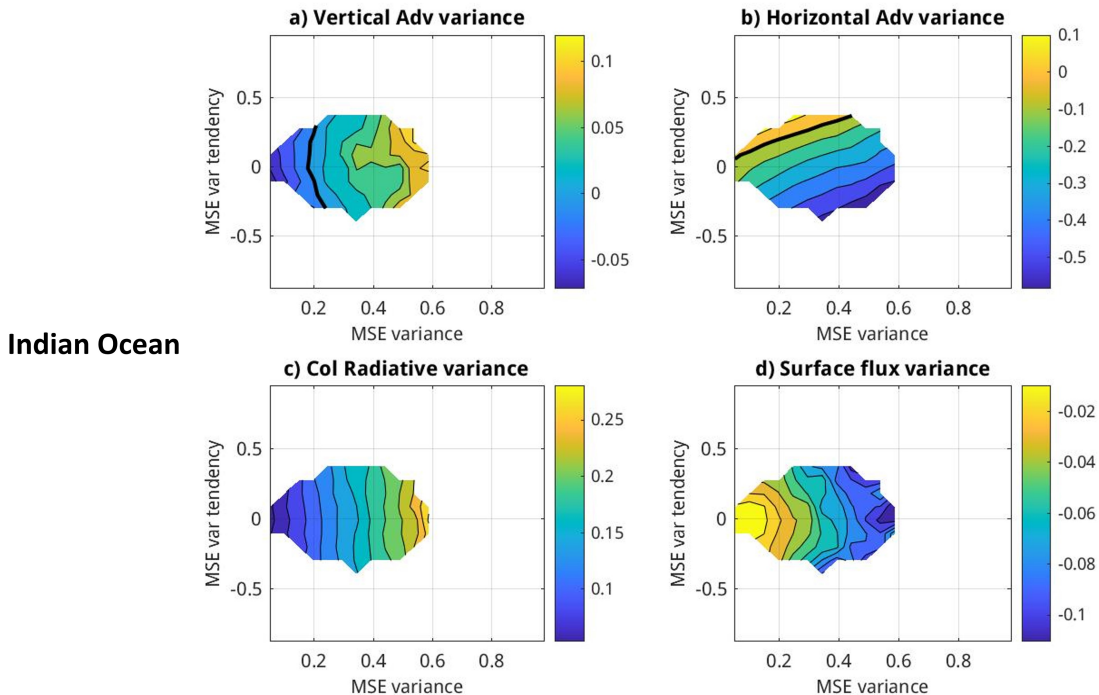


Fig. 5. Bin mean contours of the different MSE variance budget terms from Eq. 2 in the IO box showing how their contribution to MSE variance tendency varies across the variance phase space. a) contribution to variance tendency from vertical advection, b) contribution from horizontal advection, c) contribution from column radiative fluxes, and d) contribution from surface fluxes. The thick black contour represents the zero contour. c) and d) have the same sign throughout, so there is no zero contour

surface fluxes (fig. 5c) and horizontal advection (fig. 5b) act as stronger negative feedbacks when domain becomes more aggregated explaining the positive and negative contribution of these terms to maintenance of MSE variance anomalies.

Figure 6 shows the bin mean contours for the budget terms over the other three ocean basins. We observe that the behavior seen in the Indian Ocean basin is also observed qualitatively across the different regions. Changes in contour shapes between the different ocean basins lead to the difference in values observed in Fig. 4. For example, horizontal advection variance contours in the Eastern Pacific and Atlantic Ocean boxes (Fig. 6) are more horizontal as compared to the Indian Ocean or Western Pacific making its contribution to the maintenance term smaller in magnitude comparatively. This suggests that changes in magnitude of the contribution to maintenance by the horizontal advection variance term are related to subtle differences in the phase relationship between horizontal advection variance and domain MSE variance rather than an outright difference like a change in sign of the feedback. Similarly, differences in contribution to maintenance from vertical advection variance and radiative flux variance can also be associated with such subtle phase relationships. This implies that the use of the maintenance and propaga-

tion bar plots (fig. 4) to understand variance budget evolution is very sensitive to the underlying phase relationships and warrant a deeper look.

In this study, we will look at changes in horizontal and vertical advection in greater detail to understand where the observed pattern in the variance term is coming from. We particularly highlight characteristics that can explain the change in variance budget term and are similar across different regions in the tropics since those correspond to the more dominant mechanisms.

c. Changes in circulation between the most and least aggregated states

We try to better understand the physical processes behind how vertical and horizontal advection are contributing to MSE variance. To do so, we look at two things. One, how does column integrated MSE advection in the moist and dry columns change as the overall domain becomes less or more aggregated. This tells us about the maintenance of aggregation anomalies. Second, we examine how the three dimensional circulation in the domain boxes changes when the basins are most aggregated compared to when the basins are least aggregated. In figures 7 to 10, column integrated MSE advection terms and the three dimensional circulation profiles are plotted as a function

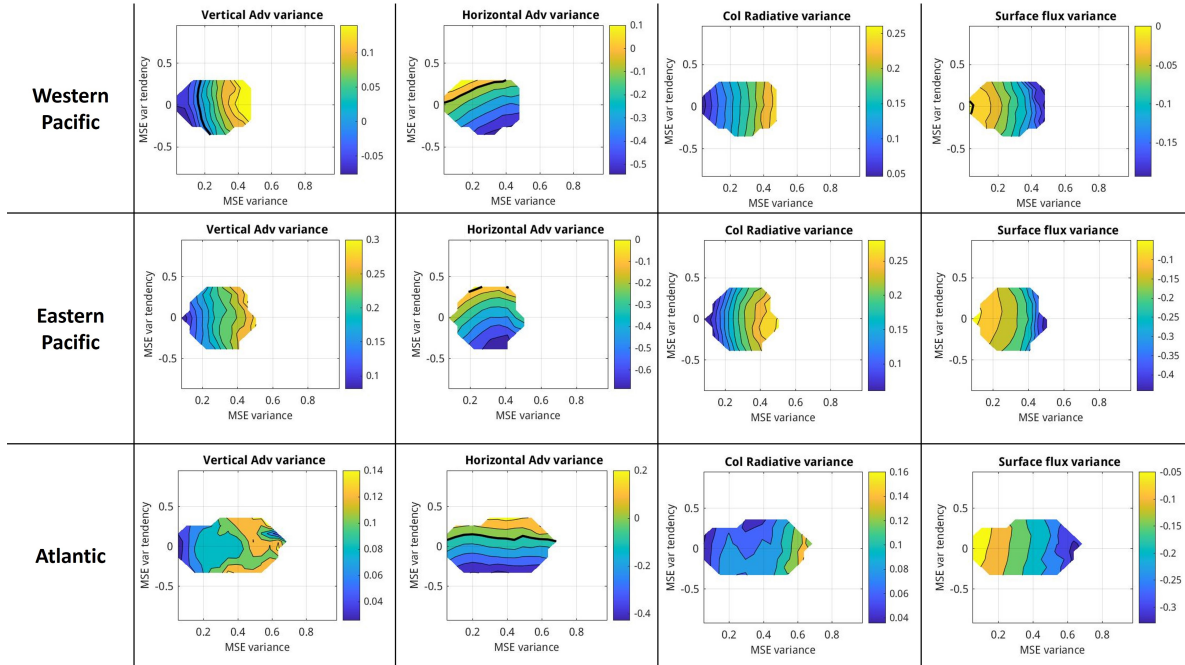


FIG. 6. Same as Fig. 5 but for other three ocean basins - Western Pacific (WP), Eastern Pacific (EP), and Atlantic Ocean (AO).

of binned column MSE. For each time step, we arrange all grid points in the domain in increasing order of column MSE, and then bin them into ten equal percentile bins to rank high MSE (which we will refer to as moist) and low MSE (dry) columns. The MSE deciles are further composited over 10% of the times when the domain is most and least aggregated to show the differences as the overall domain becomes more or less aggregated.

1) HORIZONTAL ADVECTION AND HORIZONTAL CIRCULATION CHANGES

Figure 7 shows the bin mean horizontal advection for the column MSE percentile bins in all four domains, composited for when the domain is most aggregated and when it is least aggregated. We observe that while horizontal advection is mostly negative (i.e. it has a tendency to reduce MSE in the column) across all the columns in the different region, how the values change with aggregation can differ in different columns and different basins. The moist columns in all four regions show a tendency to export more MSE out of the column by horizontal advection with stronger aggregation. This is a negative contribution of horizontal advection to maintenance of aggregation since it contributes to decreasing the variance more strongly when more aggregated (making a negative feedback more negative). In contrast, the horizontal advection tends to export less MSE out of the dry columns in Indian Ocean and Western Pacific basins, while the dry columns show a tendency for stronger advection out of the column in the Eastern Pacific and the

Atlantic Ocean basins as the domains aggregate. Reduced tendency to make the dry columns drier with aggregation is also a negative maintenance contribution since it implies increased anomalous moistening of the dry columns (making the negative feedback more negative). However, the tendency to make the dry columns drier with aggregation is a positive maintenance contribution. Therefore we will expect the maintenance term for horizontal advection to be more negative for the Indian Ocean and Western Pacific boxes. This explains the observed differences in magnitude of the maintenance term for horizontal advection in fig. 4a. It should also be noted that horizontal advection over moist columns changes uniformly with aggregation throughout the different basins while the dry regions behave differently over different ocean basins.

Next, we'll look at the changes in horizontal circulation profiles during the most and least aggregated states as a function of the binned column MSE bins (Fig. 8). The two dimensional column MSE - height space distorts the geography of the domain. Therefore, horizontal circulation has to be visualized as flow between dry and moist columns. This is calculated by computing the projection of the anomalous horizontal wind vector at each grid point in the direction of the MSE gradient. Collecting and plotting the bin mean of the projected winds then represents the anomalous horizontal winds in the direction of more moist columns at each location in the bin.

Looking at panels a and b in figure 8, we observe that when the domain is least aggregated (panel b), the anoma-

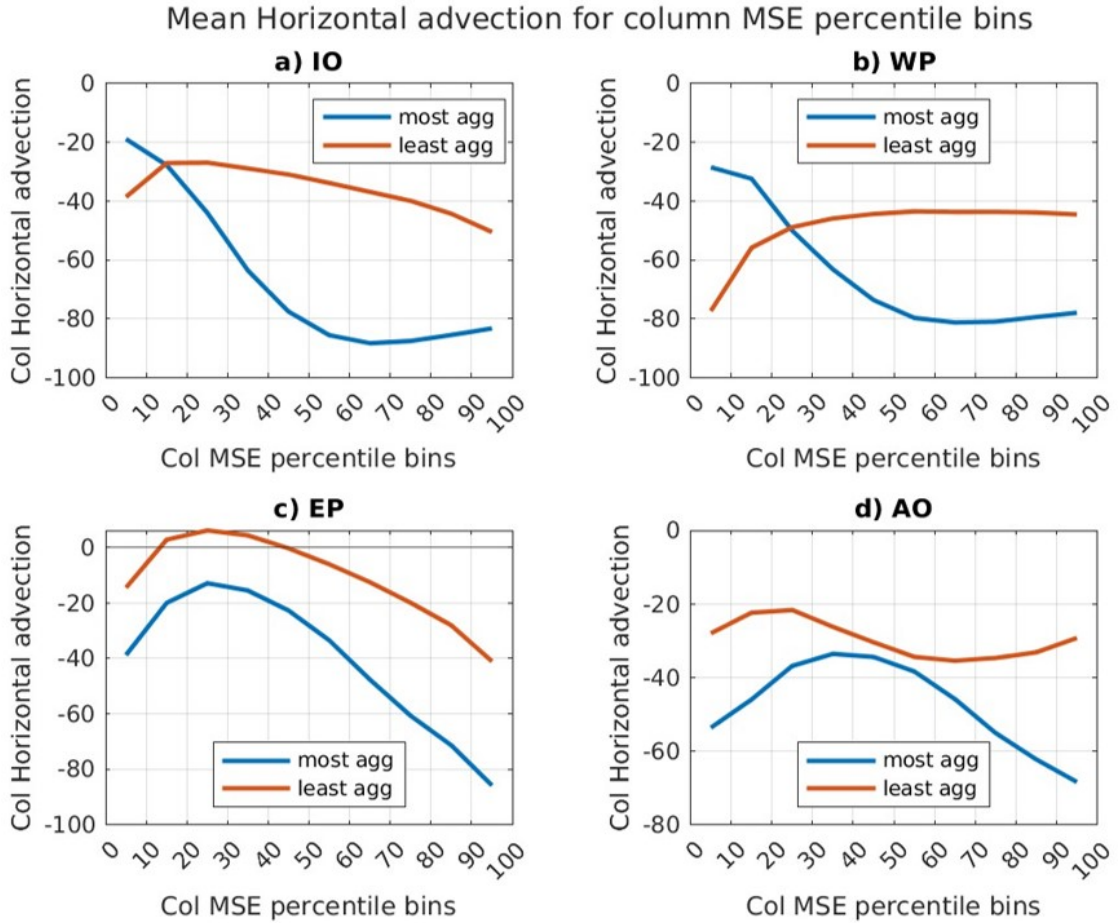


Fig. 7. Bin mean column integrated horizontal MSE advection for deciles of column MSE in all four ocean boxes when the domain is most aggregated (blue) and when it is least aggregated (red). X-axis represents the deciles of column MSE arranged to go from dry to moist columns as you go left to right.

lous horizontal flow is negative at lower levels, meaning that anomalous flow is from moist to dry columns. Conversely, when the domain is more aggregated, the anomalous horizontal flow is from the dry to moist columns near the surface. This indicates that extent of aggregation in the domain is linked to a reversal in direction of anomalous horizontal winds. Similar wind change patterns are observed over the other boxes as well (not shown). A recent study by Adames-Corraliza and Mayta (2023) have hypothesized that such a change in wind direction could be related to interactions between moisture gradient driven large scale organized convection and circulation in the tropics and this is discussed more in section 4.

2) VERTICAL ADVECTION AND VERTICAL VELOCITY PROFILE CHANGES

Variance due to the vertical advection was found to contribute positively to the maintenance of aggregation anomalies in figure 4. Figure. 5 showed that this happens

because as the domain becomes more aggregated, variance tendencies from vertical advection become more positive. In theory, this could be attributed to increased anomalous moistening tendency of the moist columns or increased anomalous drying tendency of the dry columns due to vertical advection. Further, these changes can be due to a combination of 1) changes in the amount of vertical motion and/or 2) changes in the top-heaviness of the vertical motion profile and/or 3) changes in thermodynamic profiles affecting vertical advection without changes in the vertical motion. We wish to diagnose which of these changes is occurring.

Previous idealized modelling studies have highlighted the important role of increased low level subsidence in dry regions being an important positive feedback for aggregation (Muller and Held 2012). In contrast, Tsai and Mapes (2022) show that ascending vertical motion profiles in the moist columns tend to be more bottom heavy for more aggregated cases over Indian Ocean in MERRA-2

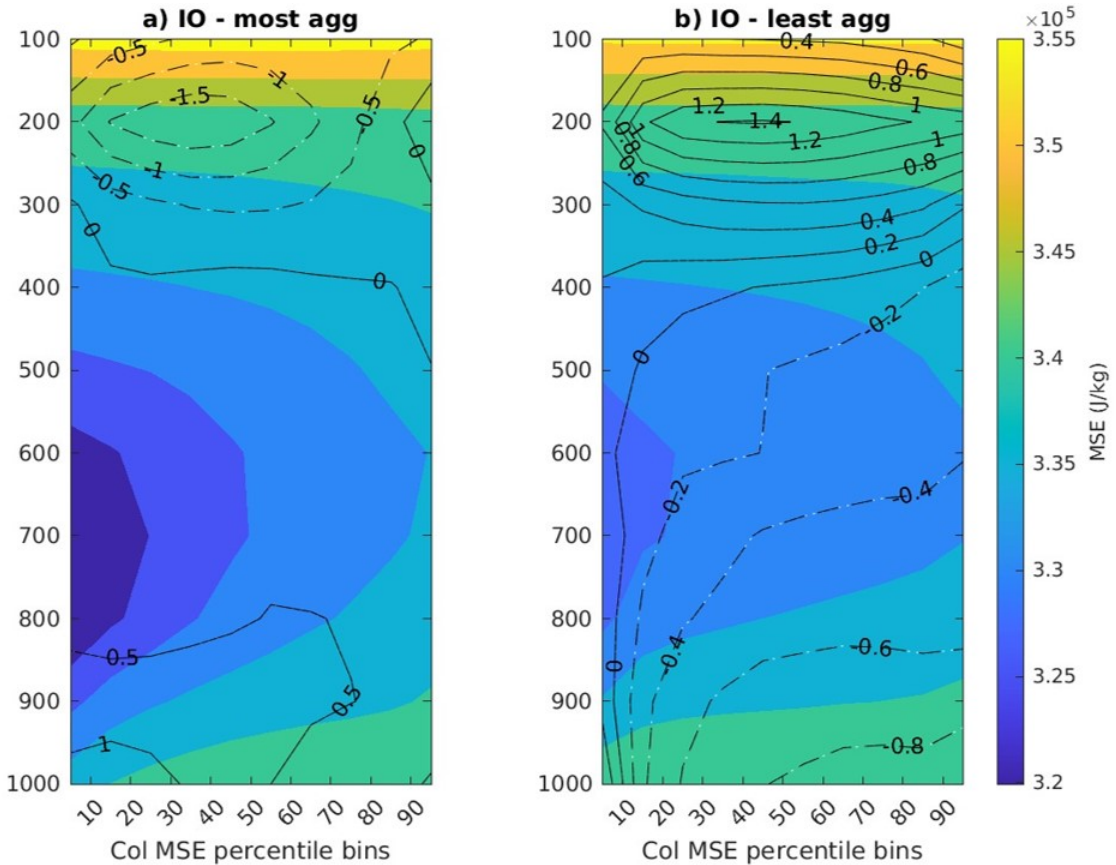


FIG. 8. Contours of anomalous horizontal winds projected on MSE gradient for IO box composited over a) 10% of the times when the domain is most aggregated, and b) 10% of the times when the domain is least aggregated. Y-axis is height in pressure units, and x-axis is the deciles of column MSE. Anomalies are computed with respect to a climatological mean state for each grid point. Solid contours mean positive value and dashed contours mean negative values. For a given column, positive contour values denote that flow is toward moister columns (to the right) and vice versa. Shading represents vertical MSE profile for the column bins.

data. However, other previous studies also discuss how geographic variability in vertical motion profile shape implies geographical differences in how convection amplifies during such cyclical modes (Inoue et al. 2021). This then raises the question, are there specific patterns in vertical motion profile shape changes which can be observed consistently across the different ocean basins that can explain the positive contribution of vertical advection to maintenance of aggregation in this framework? Are these driven by vertical motion profile changes in the dry regions or the moist regions?

Column integrated vertical advection as a function of binned column MSE and composited over 10% of the most and least aggregated cases for all four domains is shown in fig. 9a1, b1, c1, and d1. Starting off with the Indian Ocean box (fig. 9a1), we observe that the moist columns tend to lose MSE and the dry columns tend to gain MSE due to vertical advection when the domain is less aggregated. This is representative of vertical advection acting as a negative feedback on MSE anomalies when the domain is less

aggregated, consistent with fig. 5a. Further, we observe that the moist columns tend to be dried more by vertical advection as the domain becomes more aggregated. This is a negative maintenance contribution as this tends to make a negative feedback more negative. However, dry columns tend to be moistened less by vertical advection at the same time, which is a positive contribution to the maintenance term. Since the total maintenance for vertical advection is positive in the Indian Ocean box as per fig. 4a, vertical advection changes in the dry columns must be dominating over the changes in moist columns.

This change in vertical advection as the domain becomes more aggregated can also be visualized by plotting the difference between the two lines in fig. 9a1. This difference is plotted in fig. 9a2 in black, which shows the least aggregated case subtracted from the most aggregated case. Negative values denote anomalous drying tendency of the column as domain aggregates and positive values denote anomalous moistening tendency. Comparing figures for Indian Ocean box with the other domains (fig. 9 b,c, and

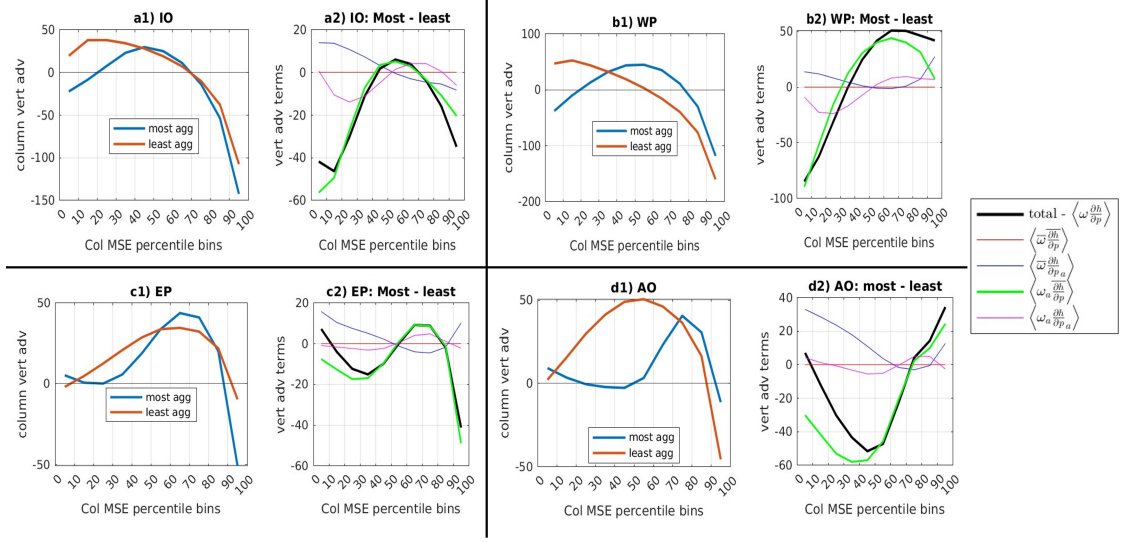


Fig. 9. a1), b1), c1), d1) - Bin mean column integrated vertical advection for deciles of column MSE when the domain is most aggregated (blue) and when it is least aggregated (red) for IO, WP, EP, AO domains respectively. a2), b2), c2), d2) - Black curve represents the differences in total column vertical advection for a given column MSE bin between most and least aggregated cases for each basin. Other colors represent the differences for various terms in vertical advection decomposition as per Eq. 5.

d), we observe that while the shape of the vertical advection curve itself can be different between the different domain, all domains show an anomalous drying or a weakened moistening tendency over the dry columns with aggregation due to changes in vertical advection. We also observe that moist columns in Indian Ocean and Eastern Pacific show a stronger anomalous drying tendency as vertical advection changes with aggregation. However, for the Western Pacific and Atlantic Ocean boxes, the moist columns show an increased anomalous moistening tendency in the moist columns with aggregation due to vertical advection. This discrepancy suggests that vertical advection changes in the dry or the subsiding columns are more uniform across the different regions. Moreover, since vertical advection overall contributes positively to maintenance of aggregation in all ocean basins (fig. 4a), these changes over dry columns can be very important to understanding the physical response.

To better understand whether these changes in vertical advection come from changes in vertical motion profile or from changes in the MSE profile, we decompose vertical advection within each bin as follows:

$$\left\langle \omega \frac{\partial h}{\partial p} \right\rangle = \left\langle \overline{\omega \frac{\partial h}{\partial p}} \right\rangle + \left\langle \overline{\omega \frac{\partial h}{\partial p_a}} \right\rangle + \left\langle \overline{\omega_a \frac{\partial h}{\partial p}} \right\rangle + \left\langle \overline{\omega_a \frac{\partial h}{\partial p_a}} \right\rangle \quad (5)$$

In this equation, the overbar denotes a time average across the most and least aggregated times and the subscript 'a' represents anomaly from the time mean. The difference between the most and least aggregated states for

the decomposed terms are plotted as colored thin lines in figure 9a2, b2, c2, and d2. Since the mean profiles are constant between the most and least aggregated states, the line corresponding to $\langle \overline{\omega \frac{\partial h}{\partial p}} \rangle$ is zero (red). We observe that change in total vertical advection is very closely followed by change in $\langle \overline{\omega_a \frac{\partial h}{\partial p}} \rangle$, which corresponds to anomalous changes in vertical motion profiles acting on a time mean MSE gradient profile (green). This suggests that variability in vertical advection is mainly explained by the changes in vertical motion profiles between most and least aggregated states. This is observed robustly over all four ocean domains.

Figure 10a shows the vertical profiles of mean vertical velocity (contour) and mean MSE (shading) in the left most panel, and anomalous vertical velocity (contour) and anomalous MSE (shading) during the most and least aggregated cases in the other two panels for the Indian Ocean domain. As expected we observe that the mean vertical velocity is ascending over the moist columns and descending over the dry columns. We further observe that the negative MSE anomalies over the drier columns dominate the MSE profile changes as shown by the range of color shading when the domain is most aggregated. The MSE increase in the moist columns is comparatively closer to zero. In terms of vertical velocity changes, we observe a strong increase in upward vertical velocity over the moist columns with stronger aggregation in the domain. We also observe a stronger low level subsidence over the dry regions consistent with previous idealized modeling studies. This increase in subsidence combined with the positive

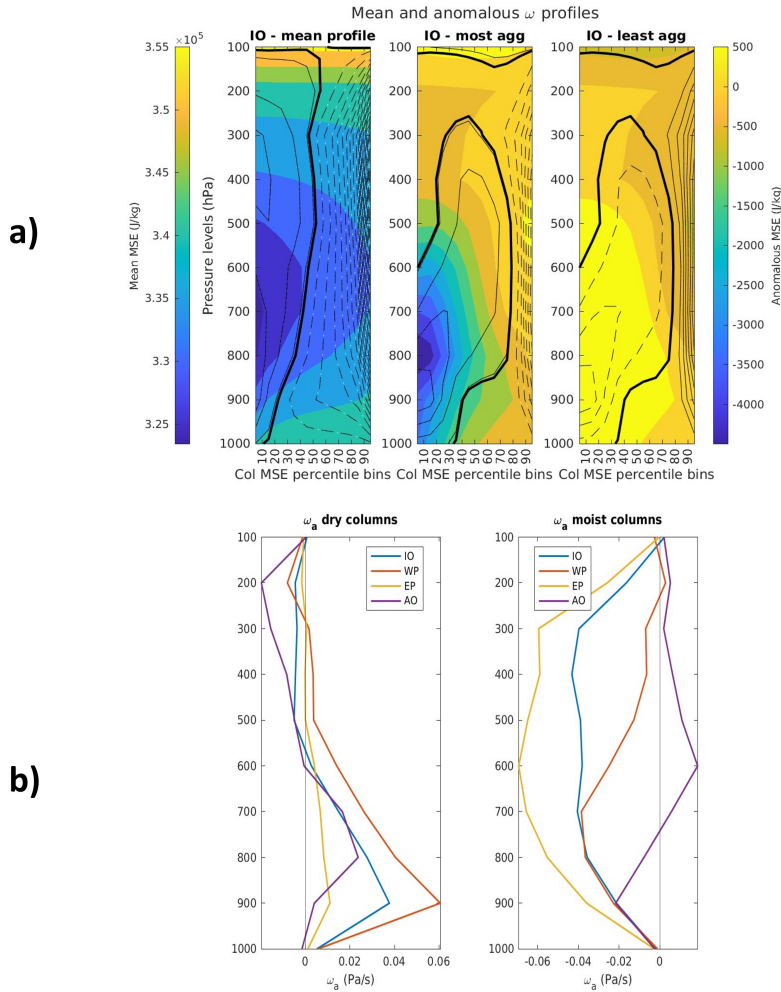


FIG. 10. a) Mean and anomalous vertical velocity in Pa/s (contours), and MSE in J/kg (shading) for the different column MSE deciles in Indian Ocean domain. Mean and anomalies consistent with definitions for Eq. 5. Panels showing composite over the most and least aggregated cases shows anomalies with respect to the mean profile. Thick black contour corresponds to the zero contour in all panels. Solid contours represent positive mean/ anomaly. Dashed contours represent negative mean/ anomaly. Contour levels are spaced every $0.01 Pa/s$ for the mean profile and every $0.005 Pa/s$ for the anomalous profiles. Left colorbar is for the mean MSE shading and right colorbar is for the anomalous MSE shading. b) anomalous vertical velocity profiles in all four ocean basins over the two driest deciles (left) and two moistest deciles (right).

vertical MSE gradient at low levels contributes to anomalous negative advection or anomalous drying of the dry columns. This anomalous drying causes the weakening in the moistening tendency over the dry columns discussed above. In contrast, it is not easy to make out if the enhancement of upward vertical velocity over the moistest columns is bottom or top heavy.

Vertical velocity profile changes are better visualized in panel b in fig. 10 which shows the anomalous vertical motion profile for the two driest and two moistest bins from panel a. The anomalous vertical velocity plotted here is the difference between the most and least aggregated composites. Profiles from all four ocean basins are plotted for easy comparison. Fig. 10b clearly shows a ubiquitous increase in low level subsidence in the dry columns in all

ocean basins with aggregation. In contrast, changes over the moistest columns are not uniform. We observe that enhancement of upward motion has a relatively more bottom heavy profile in the Western Pacific and Atlantic Ocean as compared to Indian Ocean and Eastern Pacific. Bottom heavy ascent can be associated with decreased drying tendency due to vertical advection in the moist columns in Western Pacific and Atlantic Ocean, whereas the relatively more top heavy ascent strengthens the vertical advective drying tendency of the moist columns in Indian Ocean and Eastern Pacific basins. These differences in the moist regions are consistent with changes observed in fig. 9.

Idealized modeling studies can disagree on what causes the increase of low level subsidence in dry regions. Muller and Held (2012) found this to be driven by enhanced low

level radiative cooling in dry regions, whereas (Holloway and Woolnough 2016) found the low level circulation to not be driven by radiative changes in their simulation. Understanding the exact relationship between vertical radiative cooling profiles and its impact on circulation and organization of convection is an open area of current research. Our results support that such feedbacks are important for understanding maintenance of large-scale aggregation anomalies.

4. Summary and Discussions

This study aims to establish a process oriented framework to visualize and understand the aggregation of convection in the real world. To do so, we utilized the spatial variance of MSE over ocean-wide large domains as our metric of aggregation. Defining aggregation based on the spatial variance of MSE allows us to focus on aggregation in terms of its impact on the large-scale environment, providing a different perspective to the one obtained from studying aggregation through characterization of cloud organization. Also, the domain sizes in this study are much bigger than the $10^\circ \times 10^\circ$ boxes used in previous work. This shifts the focus from aggregation at meso-scales to aggregation at larger scales in this study.

We develop a new phase space to visualize the evolution of aggregation in the form of the MSE variance phase space. This framework puts domain MSE variance on the x-axis (extent of aggregation) and the tendency of MSE variance on y-axis (changes in aggregation). A composite vector plot showing the evolution of aggregation on this phase space highlights that aggregation in the real world is a transient process in the form of continuous aggregation-disaggregation cycles (fig. 2). This visualization naturally encourages thinking about aggregation in real world as a cyclical mode compared to thinking of aggregation as a one-way process or as a quasi-stationary equilibrium state based on the idealized model results.

Different terms of the MSE variance budget (Eq. 2) represent the different processes that can contribute to aggregation or disaggregation. The different terms include variance from vertical advection, horizontal advection, radiative fluxes and surface fluxes. In this study, we focus on how these processes contribute to the maintenance and propagation of the above mentioned aggregation-disaggregation cycles. This is different from previous notions of maintenance of aggregation which focus more on maintenance of the mean aggregated state, while here we focus on maintenance of aggregation anomalies about the mean state. Contribution to propagation of the cycle represents what determines when the domain aggregates and disaggregates.

Key features observed throughout different regions in the tropics are listed below.

- For the mean state (Fig. 3), we find surface fluxes and horizontal advection tend to resist aggregation, while radiative fluxes tend to support aggregation throughout the tropics. Further, vertical advection does not tend to resist aggregation. It either tends to support aggregation or have close to zero impact on the mean aggregated state in the different basins. Contributions to the mean state are broadly consistent with previous idealized modeling studies.
- Our results highlight that only the variance from horizontal advection plays a role in determining when the domain aggregates and disaggregates (Fig. 4b). Hence, horizontal advection acts as a driver for aggregation-disaggregation cycles. All four budget terms have a significant role in contributing to the strength of aggregation anomalies.

Contribution to the strength of aggregation anomalies is related to how the budget term feedbacks onto aggregation. We find that surface fluxes and horizontal advection tend to dampen aggregation anomalies more strongly with larger anomalies, while radiative fluxes and vertical advection tend to amplify aggregation anomalies more strongly (Fig. 4a). We explore the advective feedbacks in greater detail in this study. However, based on previous studies we expect increased air-sea enthalpy disequilibrium over the dry regions during a more aggregated state to drive stronger moistening tendencies by surface fluxes which will tend to dampen the aggregation anomaly (Wing and Emanuel 2014; Pope et al. 2023). For radiative fluxes, we expect increased high clouds and water vapor in the moist regions to drive increased moistening which will tend to amplify the aggregation anomaly (Pope et al. 2021, 2023).

We show that vertical advection broadly tends to moisten the dry columns in the domain. However, as the domain becomes more aggregated, we observe that vertical advection tends to moisten the dry columns less as compared to the least aggregated states (Fig. 9). This tends to support the existing aggregation anomalies in the domain. While the change in vertical advection over the dry columns is qualitatively consistently over all ocean basins, changes over the moist columns can differ between the different regions. Looking at the vertical velocity profiles reveals that the low level subsidence over the drier columns is enhanced across all ocean basins when the domain is more aggregated which supports the weakening tendency to moisten the drier columns (Fig. 10). Moist columns instead show differences in top heaviness of the enhanced ascending profiles in different basins which can explain why changes in vertical advection are not consistent across the basins over different basins. Since the overall effect on variance by changes in vertical advection qualitatively matches with the effect of changes over the dry columns, we expect the response in dry columns to be the more dominant mechanism.

Similarly, we observe that horizontal advection tends to dry the moist columns more strongly as the domain becomes more aggregated in all ocean basins (Fig. 7). In contrast, changes in horizontal advection over the dry columns are not consistent across the ocean basins. However, the increased drying tendencies over the moist columns in more aggregated states is larger in magnitude and explains the increased tendency to damp the aggregation anomalies by horizontal advection. The three-dimensional structure of the horizontal circulation shows that anomalous horizontal circulation changes in direction with aggregation. The anomalous horizontal flow is from the dry to moist columns in lower levels when the domain is more aggregated, and is from moist to dry columns when the domain is less aggregated.

Observation about the change in horizontal wind direction in this study is also consistent with recent studies presenting observational and theoretical evidence for horizontal moisture gradient driven moisture modes (Mayta and Adames-Corraliza 2023; Adames-Corraliza and Mayta 2023). Similar to aggregation - disaggregation cycles, these moisture modes were also found to be driven by horizontal advection. As per this theory, presence of strong moisture gradients in the domain spins up moisture mode eddies which act to even out the moisture mode gradient (Adames-Corraliza and Mayta 2023). Therefore, the existence of strong eddy flow from moist to dry columns should lead to small moisture gradients and a less aggregated domain, while the absence of eddy flow should lead to build up of strong moisture gradients and a more aggregated state. This could be a possible hypothesis for how horizontal advection can be driving the propagation of the aggregation-disaggregation cycles and explain the structure of horizontal circulation we observe in our results. If true, this suggests that large-scale aggregation being observed here can be thought of in terms of a strong ITCZ or Hadley cell circulation. Other non planetary scale moisture modes then act as a disaggregation process. This could be a significant change in how we think about aggregation manifesting in the real world because traditionally moisture modes were thought to be an example of aggregation in the real world and not a part of the disaggregation process. This also implies that aggregation at relatively smaller scales like meso-scales within these wave modes need not match with the state of aggregation at larger scales, making the spatial scale of aggregation critically important when comparing different studies and metrics.

Another interesting aspect of these results are the similarities and differences with the expectations based on idealized model studies. Our results show that while radiative fluxes are important for maintenance of aggregation-disaggregation cycles, that does not mean that they control when the domain will aggregate or disaggregate. Rather, that is governed by horizontal advection. Therefore, understanding horizontal advection and how that may change

with climate change will be an important factor in understanding aggregation under a changing climate, particularly the frequency of aggregation. Wing (2019) discuss how frequency of aggregation is important for its impact on climate and extreme precipitation events in the real world. The aggregation-disaggregation cycles we study in this work are expected to be relevant for understanding the aggregation that is associated with precipitation extremes since these are expected to be associated with anomalously aggregated conditions. Hence, these aggregation-disaggregation cycles are worthy of further study.

Acknowledgments. This work has been supported in part by funding from National Science Foundation award 1759793. Maithel would like to thank Victor Mayta for help with MSE budget calculations from raw ERA 5 data. Authors would also like to thank Ángel Adames-Corralliza for helpful discussions that motivated the creation of figure 8.

Data availability statement. ERA 5 data used in the study is available at <https://doi.org/10.24381/cds.bd0915c6>

References

- Adames-Corralliza, F., and V. Mayta, 2023: The Stirring Tropics: Theory of Moisture Mode/Hadley Cell Interactions. URL <https://eartharxiv.org/repository/view/5166/>, publisher: EarthArXiv.
- Andersen, J. A., and Z. Kuang, 2012: Moist Static Energy Budget of MJO-like Disturbances in the Atmosphere of a Zonally Symmetric Aquaplanet. *Journal of Climate*, **25** (8), 2782–2804, <https://doi.org/10.1175/JCLI-D-11-00168.1>, URL <https://journals.ametsoc.org/view/journals/clim/25/8/jcli-d-11-00168.1.xml>.
- Back, L. E., and C. S. Bretherton, 2006: Geographic variability in the export of moist static energy and vertical motion profiles in the tropical Pacific. *Geophysical Research Letters*, **33** (17), <https://doi.org/10.1029/2006GL026672>, URL <https://onlinelibrary.wiley.com/doi/abs/10.1029/2006GL026672>.
- Back, L. E., Z. Hansen, and Z. Handlos, 2017: Estimating Vertical Motion Profile Top-Heaviness: Reanalysis Compared to Satellite-Based Observations and Stratiform Rain Fraction. *Journal of the Atmospheric Sciences*, **74** (3), 855–864, <https://doi.org/10.1175/JAS-D-16-0062.1>, URL <https://journals.ametsoc.org/view/journals/atsc/74/3/jas-d-16-0062.1.xml>, publisher: American Meteorological Society Section: Journal of the Atmospheric Sciences.
- Bony, S., A. Semie, R. J. Kramer, B. Soden, A. M. Tompkins, and K. A. Emanuel, 2020: Observed Modulation of the Tropical Radiation Budget by Deep Convective Organization and Lower-Tropospheric Stability. *AGU Advances*, **1** (3), e2019AV000155, <https://doi.org/10.1029/2019AV000155>, URL <https://onlinelibrary.wiley.com/doi/abs/10.1029/2019AV000155>, eprint: <https://onlinelibrary.wiley.com/doi/pdf/10.1029/2019AV000155>.
- Bretherton, C. S., P. N. Blossey, and M. Khairoutdinov, 2005: An Energy-Balance Analysis of Deep Convective Self-Aggregation above Uniform SST. *Journal of the Atmospheric Sciences*, **62** (12), 4273–4292, <https://doi.org/10.1175/JAS3614.1>, URL <https://journals.ametsoc.org/view/journals/atsc/62/12/jas3614.1.xml>, publisher: American Meteorological Society Section: Journal of the Atmospheric Sciences.
- Bretherton, C. S., and M. F. Khairoutdinov, 2015: Convective self-aggregation feedbacks in near-global cloud-resolving simulations of an aquaplanet. *Journal of Advances in Modeling Earth Systems*, **7** (4), 1765–1787, <https://doi.org/10.1002/2015MS000499>, URL <https://onlinelibrary.wiley.com/doi/abs/10.1002/2015MS000499>, eprint: <https://onlinelibrary.wiley.com/doi/pdf/10.1002/2015MS000499>.
- Bretherton, C. S., M. E. Peters, and L. E. Back, 2004: Relationships between Water Vapor Path and Precipitation over the Tropical Oceans. *Journal of Climate*, **17** (7), 1517–1528, [https://doi.org/10.1175/1520-0442\(2004\)017<1517:RBWVPA>2.0.CO;2](https://doi.org/10.1175/1520-0442(2004)017<1517:RBWVPA>2.0.CO;2), URL https://journals.ametsoc.org/view/journals/clim/17/7/1520-0442_2004_017_1517_rbwvpa.2.0.co.2.xml.
- Coppin, D., and S. Bony, 2015: Physical mechanisms controlling the initiation of convective self-aggregation in a General Circulation Model. *Journal of Advances in Modeling Earth Systems*, **7** (4), 2060–2078, <https://doi.org/10.1002/2015MS000571>, URL <https://onlinelibrary.wiley.com/doi/abs/10.1002/2015MS000571>, eprint: <https://onlinelibrary.wiley.com/doi/pdf/10.1002/2015MS000571>.
- Cronin, T. W., and A. A. Wing, 2017: Clouds, Circulation, and Climate Sensitivity in a Radiative-Convective Equilibrium Channel Model. *Journal of Advances in Modeling Earth Systems*, **9** (8), 2883–2905, <https://doi.org/10.1002/2017MS001111>, URL <https://onlinelibrary.wiley.com/doi/abs/10.1002/2017MS001111>, number: 8, eprint: <https://onlinelibrary.wiley.com/doi/pdf/10.1002/2017MS001111>.
- Dirkes, C. A., A. A. Wing, S. J. Camargo, and D. Kim, 2023: Process-Oriented Diagnosis of Tropical Cyclones in Reanalyses Using a Moist Static Energy Variance Budget. *Journal of Climate*, **36** (16), 5293–5317, <https://doi.org/10.1175/JCLI-D-22-0384.1>, URL <https://journals.ametsoc.org/view/journals/clim/36/16/JCLI-D-22-0384.1.xml>, publisher: American Meteorological Society Section: Journal of Climate.
- Held, I. M., R. S. Hemler, and V. Ramaswamy, 1993: Radiative-Convective Equilibrium with Explicit Two-Dimensional Moist Convection. *Journal of the Atmospheric Sciences*, **50** (23), 3909–3927, [https://doi.org/10.1175/1520-0469\(1993\)050<3909:RCEWET>2.0.CO;2](https://doi.org/10.1175/1520-0469(1993)050<3909:RCEWET>2.0.CO;2), URL https://journals.ametsoc.org/view/journals/atsc/50/23/1520-0469_1993_050_3909_rcwet_2.0_co_2.xml, publisher: American Meteorological Society Section: Journal of the Atmospheric Sciences.
- Hersbach, H., and Coauthors, 2020: The ERA5 global reanalysis. *Quarterly Journal of the Royal Meteorological Society*, **146** (730), 1999–2049, <https://doi.org/10.1002/qj.3803>, URL <https://onlinelibrary.wiley.com/doi/abs/10.1002/qj.3803>, eprint: <https://onlinelibrary.wiley.com/doi/pdf/10.1002/qj.3803>.
- Holloway, C. E., A. A. Wing, S. Bony, C. Muller, H. Masunaga, T. S. L'Ecuyer, D. D. Turner, and P. Zuidema, 2017: Observing Convective Aggregation. *Surveys in Geophysics*, **38** (6), 1199–1236, <https://doi.org/10.1007/s10712-017-9419-1>, URL <https://doi.org/10.1007/s10712-017-9419-1>.
- Holloway, C. E., and S. J. Woolnough, 2016: The sensitivity of convective aggregation to diabatic processes in idealized radiative-convective equilibrium simulations. *Journal of Advances in Modeling Earth Systems*, **8** (1), 166–195, <https://doi.org/10.1002/2015MS000511>, URL <https://agupubs.onlinelibrary.wiley.com/doi/abs/10.1002/2015MS000511>, eprint: <https://agupubs.onlinelibrary.wiley.com/doi/pdf/10.1002/2015MS000511>.
- Inoue, K., and L. E. Back, 2017: Gross Moist Stability Analysis: Assessment of Satellite-Based Products in the GMS Plane. *Journal of the Atmospheric Sciences*, **74** (6), 1819–1837, <https://doi.org/10.1175/JAS-D-16-0218.1>, URL <https://journals.ametsoc.org/view/journals/atsc/74/6/jas-d-16-0218.1.xml>.
- Inoue, K., M. Biasutti, and A. M. Fridlind, 2021: Evidence that Horizontal Moisture Advection Regulates the Ubiquitous Amplification of Rainfall Variability over Tropical Oceans. *Journal of the Atmospheric Sciences*, **78** (2), 529–547, <https://doi.org/10.1175/JAS-D-20-0201.1>, URL <https://journals.ametsoc.org/view/journals/atsc/78/2/jas-d-20-0201.1.xml>.

- Jakob, C., M. S. Singh, and L. Jungandreas, 2019: Radiative Convective Equilibrium and Organized Convection: An Observational Perspective. *Journal of Geophysical Research: Atmospheres*, **124** (10), 5418–5430, <https://doi.org/10.1029/2018JD030092>, URL <https://onlinelibrary.wiley.com/doi/abs/10.1029/2018JD030092>, eprint: <https://onlinelibrary.wiley.com/doi/pdf/10.1029/2018JD030092>.
- Kadoya, T., and H. Masunaga, 2018: New Observational Metrics of Convective Self-Aggregation: Methodology and a Case Study. *Journal of the Meteorological Society of Japan. Ser. II*, **96** (6), 535–548, <https://doi.org/10.2151/jmsj.2018-054>, URL https://www.jstage.jst.go.jp/article/jmsj/96/6/96_2018-054_article.
- Lebsock, M. D., T. S. L'Ecuyer, and R. Pincus, 2017: An Observational View of Relationships Between Moisture Aggregation, Cloud, and Radiative Heating Profiles. *Surveys in Geophysics*, **38** (6), 1237–1254, <https://doi.org/10.1007/s10712-017-9443-1>, URL <https://doi.org/10.1007/s10712-017-9443-1>.
- Maithel, V., and L. Back, 2022: Moisture Recharge–Discharge Cycles: A Gross Moist Stability–Based Phase Angle Perspective. *Journal of the Atmospheric Sciences*, **79** (9), 2401–2417, <https://doi.org/10.1175/JAS-D-21-0297.1>, URL <https://journals.ametsoc.org/view/journals/atsc/79/9/JAS-D-21-0297.1.xml>, publisher: American Meteorological Society Section: Journal of the Atmospheric Sciences.
- Mapes, B. E., E. S. Chung, W. M. Hannah, H. Masunaga, A. J. Wimmers, and C. S. Velden, 2018: The Meandering Margin of the Meteorological Moist Tropics. *Geophysical Research Letters*, **45** (2), 1177–1184, <https://doi.org/10.1002/2017GL076440>, URL <https://onlinelibrary.wiley.com/doi/abs/10.1002/2017GL076440>, eprint: <https://onlinelibrary.wiley.com/doi/pdf/10.1002/2017GL076440>.
- Mayta, V., and F. Adames-Corraliza, 2023: The Stirring Tropics: The Ubiquity of Moisture Modes and Moisture-Vortex. URL <https://eartharxiv.org/repository/view/5167/>, publisher: EarthArXiv.
- Muller, C. J., and I. M. Held, 2012: Detailed Investigation of the Self-Aggregation of Convection in Cloud-Resolving Simulations. *Journal of the Atmospheric Sciences*, **69** (8), 2551–2565, <https://doi.org/10.1175/JAS-D-11-0257.1>, URL <https://journals.ametsoc.org/view/journals/atsc/69/8/jas-d-11-0257.1.xml>, number: 8 Publisher: American Meteorological Society Section: Journal of the Atmospheric Sciences.
- Pope, K. N., C. E. Holloway, T. R. Jones, and T. H. M. Stein, 2021: Cloud-Radiation Interactions and Their Contributions to Convective Self-Aggregation. *Journal of Advances in Modeling Earth Systems*, **13** (9), e2021MS002535, <https://doi.org/10.1029/2021MS002535>, URL <https://onlinelibrary.wiley.com/doi/abs/10.1029/2021MS002535>, eprint: <https://onlinelibrary.wiley.com/doi/pdf/10.1029/2021MS002535>.
- Pope, K. N., C. E. Holloway, T. R. Jones, and T. H. M. Stein, 2023: Radiation, Clouds, and Self-Aggregation in RCEMIP Simulations. *Journal of Advances in Modeling Earth Systems*, **15** (2), e2022MS003317, <https://doi.org/10.1029/2022MS003317>, URL <https://onlinelibrary.wiley.com/doi/abs/10.1029/2022MS003317>, eprint: <https://onlinelibrary.wiley.com/doi/pdf/10.1029/2022MS003317>.
- Sakaeda, N., and G. Torri, 2022: The Behaviors of Intraseasonal Cloud Organization During DYNAMO/AMIE. *Journal of Geophysical Research: Atmospheres*, **127** (7), e2021JD035749, <https://doi.org/10.1029/2021JD035749>, URL <https://onlinelibrary.wiley.com/doi/abs/10.1029/2021JD035749>, eprint: <https://onlinelibrary.wiley.com/doi/pdf/10.1029/2021JD035749>.
- Sobel, A. H., J. Nilsson, and L. M. Polvani, 2001: The Weak Temperature Gradient Approximation and Balanced Tropical Moisture Waves. *Journal of the Atmospheric Sciences*, **58** (23), 3650–3665, [https://doi.org/10.1175/1520-0469\(2001\)058<3650:TWTGAA>2.0.CO;2](https://doi.org/10.1175/1520-0469(2001)058<3650:TWTGAA>2.0.CO;2), URL https://journals.ametsoc.org/view/journals/atsc/58/23/1520-0469_2001_058_3650_twtgaa_2.0.co_2.xml.
- Stein, T. H. M., C. E. Holloway, I. Tobin, and S. Bony, 2017: Observed Relationships between Cloud Vertical Structure and Convective Aggregation over Tropical Ocean. *Journal of Climate*, **30** (6), 2187–2207, <https://doi.org/10.1175/JCLI-D-16-0125.1>, URL <https://journals.ametsoc.org/view/journals/clim/30/6/jcli-d-16-0125.1.xml>, publisher: American Meteorological Society Section: Journal of Climate.
- Su, H., and J. D. Neelin, 2002: Teleconnection Mechanisms for Tropical Pacific Descent Anomalies during El Niño. *Journal of the Atmospheric Sciences*, **59** (18), 2694–2712, [https://doi.org/10.1175/1520-0469\(2002\)059<2694:TMFTPD>2.0.CO;2](https://doi.org/10.1175/1520-0469(2002)059<2694:TMFTPD>2.0.CO;2), URL https://journals.ametsoc.org/view/journals/atsc/59/18/1520-0469_2002_059_2694_tmftpd_2.0.co_2.xml.
- Tobin, I., S. Bony, and R. Roca, 2012: Observational Evidence for Relationships between the Degree of Aggregation of Deep Convection, Water Vapor, Surface Fluxes, and Radiation. *Journal of Climate*, **25** (20), 6885–6904, <https://doi.org/10.1175/JCLI-D-11-00258.1>, URL <https://journals.ametsoc.org/view/journals/clim/25/20/jcli-d-11-00258.1.xml>, publisher: American Meteorological Society Section: Journal of Climate.
- Tompkins, A. M., and A. G. Semie, 2017: Organization of tropical convection in low vertical wind shears: Role of updraft entrainment. *Journal of Advances in Modeling Earth Systems*, **9** (2), 1046–1068, <https://doi.org/10.1002/2016MS000802>, URL <https://onlinelibrary.wiley.com/doi/abs/10.1002/2016MS000802>, eprint: <https://onlinelibrary.wiley.com/doi/pdf/10.1002/2016MS000802>.
- Tsai, W.-M., and B. E. Mapes, 2022: Evidence of Aggregation Dependence of 5°-Scale Tropical Convective Evolution Using a Gross Moist Stability Framework. *Journal of the Atmospheric Sciences*, **79** (5), 1385–1404, <https://doi.org/10.1175/JAS-D-21-0253.1>, URL <https://journals.ametsoc.org/view/journals/atsc/79/5/JAS-D-21-0253.1.xml>, publisher: American Meteorological Society Section: Journal of the Atmospheric Sciences.
- Wing, A. A., 2019: Self-Aggregation of Deep Convection and its Implications for Climate. *Current Climate Change Reports*, **5** (1), 1–11, <https://doi.org/10.1007/s40641-019-00120-3>, URL <https://doi.org/10.1007/s40641-019-00120-3>, number: 1.
- Wing, A. A., and T. W. Cronin, 2016: Self-aggregation of convection in long channel geometry. *Quarterly Journal of the Royal Meteorological Society*, **142** (694), 1–15, <https://doi.org/10.1002/qj.2628>, URL <https://onlinelibrary.wiley.com/doi/abs/10.1002/qj.2628>, number: 694 eprint: <https://onlinelibrary.wiley.com/doi/pdf/10.1002/qj.2628>.
- Wing, A. A., K. Emanuel, C. E. Holloway, and C. Muller, 2017: Convective Self-Aggregation in Numerical Simulations: A Review. *Surveys in Geophysics*, **38** (6), 1173–1197, <https://doi.org/10.1007/s10712-017-9408-4>, URL <http://link.springer.com/10.1007/s10712-017-9408-4>.
- Wing, A. A., and K. A. Emanuel, 2014: Physical mechanisms controlling self-aggregation of convection in idealized numerical modeling simulations. *Journal of Advances in Modeling Earth Systems*, **6** (1), 59–74, <https://doi.org/10.1002/2013MS000269>, URL <https://onlinelibrary.wiley.com/doi/abs/10.1002/2013MS000269>.

- Wing, A. A., K. A. Reed, M. Satoh, B. Stevens, S. Bony, and T. Ohno, 2018: Radiative–convective equilibrium model intercomparison project. *Geoscientific Model Development*, **11** (2), 793–813, <https://doi.org/10.5194/gmd-11-793-2018>, URL <https://gmd.copernicus.org/articles/11/793/2018/gmd-11-793-2018.html>, number: 2 Publisher: Copernicus GmbH.
- Wing, A. A., and Coauthors, 2019: Moist Static Energy Budget Analysis of Tropical Cyclone Intensification in High-Resolution Climate Models. *Journal of Climate*, **32** (18), 6071–6095, <https://doi.org/10.1175/JCLI-D-18-0599.1>, URL <https://journals.ametsoc.org/view/journals/clim/32/18/jcli-d-18-0599.1.xml>, publisher: American Meteorological Society Section: Journal of Climate.
- Wing, A. A., and Coauthors, 2020: Clouds and Convective Self-Aggregation in a Multimodel Ensemble of Radiative–Convective Equilibrium Simulations. *Journal of Advances in Modeling Earth Systems*, **12** (9), e2020MS002138, <https://doi.org/10.1029/2020MS002138>, URL <https://onlinelibrary.wiley.com/doi/abs/10.1029/2020MS002138>, eprint: <https://onlinelibrary.wiley.com/doi/pdf/10.1029/2020MS002138>.